Ersch. in: Journal of Organometallic Chemistry ; 683 (2003), 1. - S. 92-102

http://dx.doi.org/10.1016/S0022-328X(03)00443-1

^{1}H-, ^{13}C-NMR and ethylene polymerization studies of zirconocene/MAO catalysts: effect of the ligand structure on the formation of active intermediates and polymerization kinetics

Konstantin P. Bryliakov [a,b,*], Nina V. Semikolenova [a], Dmitrii V. Yudaev [a], Vladimir A. Zakharov [a], Hans H. Brintzinger [c], Martin Ystenes [d], Erling Rytter [d,e], Evgenii P. Talsi [a,b,*]

[a] *Boreskov Institute of Catalysis, Prospect Akad. Lavrentieva, 5, Novosibirsk 630090, Russia*
[b] *Natural Sciences Department, Novosibirsk State University, Novosibirsk 630090, Russia*
[c] *Fachbereich Chemie, University of Konstanz, D-78457 Konstanz, Germany*
[d] *Department of Chemical Engineering, Norwegian University of Science and Technology (NTNU), N-7491 Trondheim, Norway*
[e] *Statoil Research Centre, N-7005 Trondheim, Norway*

Abstract

Using ^{1}H- and ^{13}C-NMR spectroscopies, cationic intermediates formed by activation of L_2ZrCl_2 with methylaluminoxane (MAO) in toluene were monitored at Al/Zr ratios from 50 to 1000 (L_2 are various cyclopentadienyl (Cp), indenyl (Ind) and fluorenyl (Flu) ligands). The following catalysts were studied: (Cp-R)$_2$ZrCl$_2$ (R = Me, 1,2-Me$_2$, 1,2,3-Me$_3$, 1,2,4-Me$_3$, Me$_4$, Me$_5$, *n*-Bu, *t*-Bu), rac-ethanediyl(Ind)$_2$ZrCl$_2$, rac-Me$_2$Si(Ind)$_2$ZrCl$_2$, rac-Me$_2$Si(1-Ind-2-Me)$_2$ZrCl$_2$, rac-ethanediyl(1-Ind-4,5,6,7-H$_4$)$_2$ZrCl$_2$, (Ind-2-Me)$_2$ZrCl$_2$, Me$_2$C(Cp)(Flu)ZrCl$_2$, Me$_2$C(Cp-3-Me)(Flu)ZrCl$_2$ and Me$_2$Si(Flu)$_2$ZrCl$_2$. Correlations between spectroscopic and ethene polymerization data for catalysts (Cp-R)$_2$ZrCl$_2$/MAO (R = H, Me, 1,2-Me$_2$, 1,2,3-Me$_3$, 1,2,4-Me$_3$, Me$_4$, Me$_5$, *n*-Bu, *t*-Bu) and rac-Me$_2$Si(Ind)$_2$ZrCl$_2$ were established. The catalysts (Cp-R)$_2$ZrCl$_2$/AlMe$_3$/CPh$_3^+$B(C$_6$F$_5$)$_4^-$ (R = Me, 1,2-Me$_2$, 1,2,3-Me$_3$, 1,2,4-Me$_3$, Me$_4$, *n*-Bu, *t*-Bu) were also studied for comparison of spectroscopic and polymerization data with MAO-based systems. Complexes of type (Cp-R)$_2$ZrMe$^+$ ← Me$^-$-Al ≡ MAO (**IV**) with different [Me-MAO]$^-$ counteranions have been identified in the (Cp-R)$_2$ZrCl$_2$/MAO (R = *n*-Bu, *t*-Bu) systems at low Al/Zr ratios (50–200). At Al/Zr ratios of 500–1000, the complex [L$_2$Zr(μ-Me)$_2$AlMe$_2$]$^+$[Me-MAO]$^-$ (**III**) dominates in all MAO-based reaction systems studied. Ethene polymerization activity strongly depends on the Al/Zr ratio (Al/Zr = 200–1000) for the systems (Cp-R)$_2$ZrCl$_2$/MAO (R = H, Me, *n*-Bu, *t*-Bu), while it is virtually constant in the same range of Al/Zr ratios for the catalytic systems (Cp-R)$_2$ZrCl$_2$/MAO (R = 1,2-Me$_2$, 1,2,3-Me$_3$, 1,2,4-Me$_3$, Me$_4$) and rac-Me$_2$Si(Ind)$_2$ZrCl$_2$/MAO. The data obtained are interpreted on assumption that complex **III** is the main precursor of the active centers of polymerization in MAO-based systems.

Keywords: Metallocene catalysts; ^{1}H- and ^{13}C-NMR; Polyethylene; Structure–property relations; Transition metal chemistry

1. Introduction

Spectroscopic monitoring of the cationic intermediates formed upon activation of metallocenes with methylaluminoxane (MAO) and correlation of their concentration with polymerization activity is crucial for the elucidation of the reaction mechanisms [1–5]. Recent NMR studies [6,7] have provided important information on the structures of 'cation-like' intermediates formed upon activation of Cp_2ZrMe_2 with MAO in toluene. It was shown that complexes $Cp_2MeZr\text{-}Me \rightarrow Al \equiv MAO$ (**I**) and [$Cp_2ZrMe(\mu\text{-}Me)Cp_2ZrMe$]$^+$[Me-MAO]$^-$ (**II**) dominate in reaction solution at low Al/Zr ratios (20–50), whereas [$Cp_2Zr(\mu\text{-}Me)_2AlMe_2$]$^+$[Me-

* Corresponding authors. Present address: Boreskov Institute of Catalysis, Prospect Akad. Lavrentieva, 5, Novosibirsk 630090, Russia. Tel.: +7-3832-341877; fax: +7-3832-343766.
E-mail addresses: bryliako@catalysis.nsk.su (K.P. Bryliakov), talsi@catalysis.nsk.su (E.P. Talsi).

MAO]$^-$ (**III**) and $Cp_2ZrMe^+ \leftarrow Me^-$-Al ≡ MAO (**IV**) are the major species at high Al/Zr ratios (200–4000). It has been proposed [7] that complexes $[Cp_2Zr(\mu\text{-}Me)_2Al\text{-}Me_2]^+[Me\text{-}MAO]^-$ (**III**) and $Cp_2ZrMe^+ \leftarrow Me^-$-Al ≡ MAO (**IV**) were the precursors of the active centers of polymerization. Recently, a scheme of the formation of active centers upon interaction of complex **III** with olefins has been proposed on the basis of quantum-chemical DFT calculations [8].

It is well-known that the substituents in the ligands of a zirconocene complex affect its polymerization activity [9–14]. However, there are no NMR data on the intermediates formed in the catalytic systems L_2ZrCl_2/MAO, where L_2 are various substituted cyclopentadienyl, indenyl or fluorenyl ligands. Such data are available only for $CPh_3^+B(C_6F_5)_4^-$-based systems [15,16]. So, it is important to characterize the zirconium species formed by various zirconocenes activation with MAO and to elucidate the effect of substituents and Al/Zr ratio on the concentration of species **III** and **IV**, and polymerization activity.

In this work, we have undertaken a ^{1}H- and ^{13}C-NMR spectroscopic study of the cationic intermediates formed upon activation of L_2ZrCl_2 with MAO at various Al/Zr ratios. The following catalysts were studied: $(Cp\text{-}R)_2ZrCl_2$ (R = Me, 1,2-Me_2, 1,2,3-Me_3, 1,2,4-Me_3, Me_4, Me_5, *n*-Bu, *t*-Bu), rac-ethanediyl $(Ind)_2ZrCl_2$, rac-$Me_2Si(Ind)_2ZrCl_2$, rac-$Me_2Si(1\text{-}Ind\text{-}2\text{-}Me)_2ZrCl_2$, rac-ethanediyl$(1\text{-}Ind\text{-}4,5,6,7\text{-}H_4)_2ZrCl_2$, $(Ind\text{-}2\text{-}Me)_2ZrCl_2$, $Me_2C(Cp)(Flu)ZrCl_2$, $Me_2C(Cp\text{-}3\text{-}Me)(Flu)ZrCl_2$ and $Me_2Si(Flu)_2ZrCl_2$. Correlations between spectroscopic and ethene polymerization data for catalysts $(Cp\text{-}R)_2ZrCl_2$/MAO (R = H, Me, 1,2-Me_2, 1,2,3-Me_3, 1,2,4-Me_3, Me_4, Me_5, *n*-Bu, *t*-Bu) and rac-$Me_2Si(Ind)_2ZrCl_2$/MAO were observed. The catalysts $(Cp\text{-}R)_2ZrCl_2/AlMe_3/CPh_3^+B(C_6F_5)_4^-$ (R = Me, 1,2-Me_2, 1,2,3-Me_3, 1,2,4-Me_3, Me_4, *n*-Bu, *t*-Bu) were also studied for comparison of spectroscopic and polymerization data with MAO-based systems.

2. Experimental

2.1. Materials

Toluene and toluene-d_8 ($CD_3C_6D_5$) were dried over molecular sieves (4 Å), purified by refluxing over sodium metal and distillation in dry argon. The distilled solvents were degassed in vacuo and then stored and handled in vacuo. All experiments were carried out in sealed high-vacuum systems using break seal techniques to avoid undesired contact with the atmosphere.

L_2ZrCl_2 and $(Cp\text{-}n\text{-}Bu)_2ZrMe_2$ samples purchased from Boulder Scientific Co. were used without further purification as solutions in toluene-d_8 ([Zr] = 0.05–0.00005 M).

MAO samples were prepared from commercial MAO (Witco) by removal of the solvent and free $AlMe_3$ in vacuo at 20 °C. The solid product obtained (polymeric MAO with total Al content of 40 wt.% and Al as residual $AlMe_3$ ca. 5 wt.%) was used for the preparation of the samples.

$AlMe_3$ was purchased from Witco and used as solutions in toluene-d_8 (0.1–0.02 M).

2.2. Preparation of L_2ZrCl_2/MAO and $L_2ZrCl_2/AlMe_3/CPh_3^+B(C_6F_5)_4^-$ samples for NMR investigation

Calculated quantities of L_2ZrCl_2 solution (in toluene for ^{13}C and in toluene-d_8 for ^{1}H measurements) and MAO or $AlMe_3/CPh_3^+B(C_6F_5)_4^-$ were combined under vacuum in NMR tubes (5 and 10 mm) and the tubes were sealed off from the vacuum line. The data on Al and Zr concentrations and Al/Zr ratios of the samples prepared are given.

2.3. NMR measurements

^{1}H spectra were recorded using pulsed FT-NMR technique on Bruker DPX-250 (at 250.13 MHz) and DPX-400 NMR (at 400.13 MHz) spectrometers in cylindrical 5 mm glass sample tubes. ^{13}C spectra were recorded at 100.614 MHz, using pulsed FT-NMR technique, on a Bruker MSL-400 NMR spectrometer in cylindrical 10 mm glass sample tubes. Operating conditions: sweep width, 25 kHz (^{13}C) and 5 kHz (^{1}H); spectrum accumulation frequency used, 0.2 Hz (^{1}H) and 0.2–0.02 Hz (^{13}C); number of transients, 1000–10 000 (^{13}C) and 100–10 000 (^{1}H); 45° pulse at 10 μs (^{13}C) and 10–20° pulse at 1–2 μs (^{1}H). The data were accumulated with 16–32K data points in the time domain. Chemical shifts were measured in ppm, with positive values in the low-field direction. For calculations of ^{1}H and ^{13}C chemical shifts, the resonance of the CD_2H group of the toluene solvent was taken as 2.09 ppm (^{1}H) and that of the CD_3 group as 22.1 ppm (^{13}C).

2.4. ^{1}H-NMR spectra of L_2ZrCl_2 and $L_2ZrClMe$

For the assignment of the ^{1}H-NMR peaks of zirconium species formed in the $(Cp\text{-}R)_2ZrCl_2$/MAO systems, ^{1}H-NMR spectra of $(Cp\text{-}R)_2ZrCl_2$, $(Cp\text{-}R)_2ZrClMe$ and $[(Cp\text{-}R)_2Zr(\mu\text{-}Me)_2AlMe_2]^+[B(C_6F_5)_4]^-$ (R = Me, 1,2-Me_2, 1,2,3-Me_3, 1,2,4-Me_3, Me_4, *t*-Bu, *n*-Bu) were recorded. Complexes $(Cp\text{-}R)_2ZrClMe$ were prepared in situ via reaction of $(Cp\text{-}R)_2ZrCl_2$ with $AlMe_3$ in toluene-d_8 at 20 °C (Al/Zr = 50). ^{1}H-NMR spectra of the resulting solutions exhibit peaks of the initial zirconocene dichloride and those of the monomethylated product (Table 1). Cationic complexes $[(Cp\text{-}R)_2Zr(\mu\text{-}Me)_2AlMe_2]^+[B(C_6F_5)_4]^-$ were prepared in situ via the reaction of $(Cp\text{-}R)_2ZrCl_2$ with $AlMe_3/CPh_3^+B(C_6F_5)_4^-$

Table 1
^{1}H-NMR signals of complexes (Cp-R)$_2$ZrCl$_2$ and (Cp-R)$_2$ZrClMe (R = Me, 1,2-Me$_2$, 1,2,3-Me$_3$, 1,2,4-Me$_3$, Me$_4$, *n*-Bu, *t*-Bu)

Species	Cp	Cp-Me	Zr-Me
(Cp-Me)$_2$ZrCl$_2$	5.71 (tq, 4), J_{HH} = 2.6 and 0.5 Hz; 5.61 (t, 4), J_{HH} = 2.6 Hz	2.09 (s, 6)	
(Cp-*n*-Bu)$_2$ZrCl$_2$	5.72 (t, 4), 5.85 (t, 4), J_{HH} = 2.6 Hz		
(Cp-*n*-Bu)$_2$ZrMe$_2$	5.51 (t, 4), 5.72 (t, 4), J_{HH} = 2.6 Hz		−0.15 (s, 6)
(Cp-*t*-Bu)$_2$ZrCl$_2$	5.76 (t, 4), 6.05 (t, 4), J_{HH} = 2.7 Hz		
(Cp-1,2-Me$_2$)$_2$ZrCl$_2$	5.57 (d, 4), J_{HH} = 2.9 Hz; 5.45 (t, 2), J_{HH} = 2.9 Hz	1.94 (s, 12)	
(Cp-1,2,3-Me$_3$)$_2$ZrCl$_2$	5.31 (s, 4)	1.88 (s, 12), 1.90 (s, 6)	
(Cp-1,2,4-Me$_3$)$_2$ZrCl$_2$	5.58 (s, 4)	1.87 (s, 6), 1.83 (s, 12)	
(Cp-Me$_4$)$_2$ZrCl$_2$	5.26 (s, 2)	1.94 (s, 12), 1.70 (s, 12)	
(Cp-Me$_5$)$_2$ZrCl$_2$		1.74 (s, 30)	
(Cp-Me)$_2$ZrClMe	5.65 (t, 4), 5.48 (m, 4), J_{HH} = 2.7 Hz	1.96 (s, 6)	0.31 (s, 3)
(Cp-*n*-Bu)$_2$ZrClMe	5.55 (m, 4), 5.75 (m, 4)		0.38 (s, 3)
(Cp-*t*-Bu)$_2$ZrClMe	5.50 (m, 4), 5.87 (m, 4)		0.51 (s, 3)
(Cp-1,2,3-Me$_3$)$_2$ZrClMe	5.22 (d, 2), 4.99 (d, 2), J_{HH} = 2.7 Hz	1.76 (s, 12), 1.88 (s, 6)	−0.04 (s, 3)
(Cp-1,2,4-Me$_3$)$_2$ZrClMe	5.36 (d, 2), 5.40 (d, 2), J_{HH} = 2.7 Hz	1.74 (s, 12), 1.80 (s, 6)	0.21 (s, 3)

in toluene-d_8 in a ratio of 1:50:1 at 20 °C. In this case, only the stable complexes [(Cp-R)$_2$Zr(μ-Me)$_2$AlMe$_2$]$^+$[B(C$_6$F$_5$)$_4$]$^-$ (R = Me, 1,2-Me$_2$, 1,2,3-Me$_3$, 1,2,4-Me$_3$, Me$_4$, *t*-Bu, *n*-Bu) are observed in the reaction solution. Their NMR parameters are presented below in the corresponding sections. For the assignment of the ^{1}H-NMR peaks of [L$_2$Zr(μ-Me)$_2$AlMe$_2$]$^+$[Me-MAO]$^-$, where L$_2$ are various indenyl and fluorenyl ligands, corresponding NMR spectra were compared with those for complexes [L$_2$Zr(μ-Me)$_2$AlMe$_2$]$^+$[B(C$_6$F$_5$)$_4$]$^-$ and [L$_2$Hf(μ-Me)$_2$AlMe$_2$]$^+$[B(C$_6$F$_5$)$_4$]$^-$ available in the literature [15].

2.5. Ethylene polymerization

2.5.1. (Cp-R)$_2$ZrCl$_2$/MAO systems

The 1-l reactor was evacuated at 70 °C, cooled to 20 °C and charged with 150 ml of toluene solution containing calculated quantities of (Cp-R)$_2$ZrCl$_2$ and MAO. The zirconocene concentration in the reactor was 1.5×10^{-5} M. After the polymerization temperature had stabilized (70 °C), ethylene was introduced into the reactor (2 or 5 atm). During the polymerization time (15 min), ethylene pressure and temperature were maintained constant. The experimental unit was equipped with automatic computer-controlled system for ethylene feed, recording the ethylene consumption and providing the kinetic curve output both in the form of a table and as a graph. Catalysts initial activities (see Tables 2–5) were calculated from the ethylene consumption for the first 5 min of polymerization.

2.5.2. (Cp-R)$_2$ZrCl$_2$/AlMe$_3$/CPh$_3^+$B(C$_6$F$_5$)$_4^-$ systems

Polymerization runs were performed in a 0.2-l reactor. The reactor was evacuated at 70 °C and cooled to 20 °C. Toluene solutions containing calculated quantities of (Cp-R)$_2$ZrCl$_2$ and AlMe$_3$ were mixed under vacuum with a toluene solution of CPh$_3^+$B(C$_6$F$_5$)$_4^-$ and immediately introduced into the reactor (total volume: 70 ml; zirconocene concentration in the reactor: 1.4×10^{-5} M; components molar ratio of Zr:AlMe$_3$:B = 1:100:1). Then, the polymerization temperature (50 °C) and ethylene pressure (3 atm) were adjusted and kept constant during the polymerization time (15 min). Catalysts' initial activities (see Table 8) were calculated from the ethylene consumption for the first 5 min of polymerization.

3. Results and discussion

3.1. Spectroscopic and polymerization studies of the catalytic systems (Cp-R)$_2$ZrCl$_2$/MAO (R = Me, n-Bu, t-Bu)

In order to elucidate the effect of the structure of alkyl substituent on the concentration of species **III** and **IV**, and polymerization activity, the catalytic systems (Cp-R)$_2$ZrCl$_2$/MAO (Me, *n*-Bu, *t*-Bu) were studied at various Al/Zr ratios. We begin the analysis of experimental data with the system (Cp-*n*-Bu)$_2$ZrCl$_2$/MAO, since for this system the most detailed spectroscopic data were obtained.

3.1.1. (Cp-n-Bu)$_2$ZrCl$_2$/MAO

The formation of complexes **III**, **IV** and other zirconium species present in the catalytic system studied at various Al/Zr ratios was monitored by recording the corresponding ^{1}H-NMR resonances of their Cp rings (Fig. 1). The assignment of ^{1}H-NMR resonances of **III** was made by comparison with those observed for [(Cp-*n*-Bu)$_2$Zr(μ-Me)$_2$AlMe$_2$]$^+$[B(C$_6$F$_5$)$_4$]$^-$ (Table 2). The ^{1}H-NMR chemical shifts of the hydrogen atoms of the Cp rings of the latter complex (two pseudotriplets at

Table 2
^{1}H-NMR signals of $[(Cp\text{-}R)_2Zr(\mu\text{-}Me)_2AlMe_2]^+[B(C_6F_5)_4]^-$ and $[(Cp\text{-}R)_2Zr(\mu\text{-}Me)_2AlMe_2]^+[Me\text{-}MAO]^-$ (**III**) complexes (R = H, Me, *n*-Bu, *t*-Bu)

Species	Cp	μ-Me	Al-Me
$[Cp_2Zr(\mu\text{-}Me)_2AlMe_2]^+[Me\text{-}MAO]^-$	5.50 (s, 10)	−0.27 (s, 6)	−0.58 (s, 6)
$[(Cp\text{-}Me)_2Zr(\mu\text{-}Me)_2AlMe_2]^+[Me\text{-}MAO]^-$	5.38 [a]	NF	NF
$[(Cp\text{-}n\text{-}Bu)_2Zr(\mu\text{-}Me)_2AlMe_2]^+[Me\text{-}MAO]^-$	5.56 (t, 4), 5.62(t, 4), $J_{HH} = 2.6$ Hz	−0.23 (s, 6)	−0.54 (s, 6)
$[(Cp\text{-}t\text{-}Bu)_2Zr(\mu\text{-}Me)_2AlMe_2]^+[Me\text{-}MAO]^-$	5.59 (t, 4), 6.00 (t, 4), $J_{HH} = 2.6$ Hz	NF	NF
$[Cp_2Zr(\mu\text{-}Me)_2AlMe_2]^+[B(C_6F_5)_4]^-$	5.44 (s, 10)	−0.40 (s, 6)	−0.73 (s, 6)
$[(Cp\text{-}Me)_2Zr(\mu\text{-}Me)_2AlMe_2]^+[B(C_6F_5)_4]^-$	5.37 (t, 4), 5.46 (t, 4), $J_{HH} = 2.6$ Hz	−0.19 (s, 6)	−0.70 (s, 6)
$[(Cp\text{-}n\text{-}Bu)_2Zr(\mu\text{-}Me)_2AlMe_2]^+[B(C_6F_5)_4]^-$	5.62 (t, 4), 5.68 (t, 4), $J_{HH} = 2.6$ Hz	−0.21 (s, 6)	−0.61 (s, 6)
$[(Cp\text{-}t\text{-}Bu)_2Zr(\mu\text{-}Me)_2AlMe_2]^+[B(C_6F_5)_4]^-$	5.54 (t, 4), 6.04 (t, 4), $J_{HH} = 2.6$ Hz	−0.18 (s, 6)	−0.47 (s, 6)

NF, not found.
[a] Broad singlet ($\Delta\nu_{1/2} = 6$ Hz).

$\delta = 5.62$ and 5.68, $J_{HH} = 2.6$ Hz) were close to those of **III** formed in the system (Cp-*n*-Bu)$ZrCl_2$/MAO ($\delta =$ 5.56 and 5.62, $J_{HH} = 2.6$ Hz) (Fig. 1a, Table 2).

The ^{1}H-NMR spectrum in the range of Cp hydrogen atoms of the system (Cp-*n*-Bu)$_2ZrCl_2$/MAO ([(Cp-*n*-Bu)$_2ZrCl_2$] = 0.01 M, Al/Zr = 50) in toluene displays peaks of complex **III**, whereas several signals denoted by symbols $\mathbf{IV}_1$, $\mathbf{IV}_2$ and $\mathbf{IV}_3$ (Fig. 1a) are assigned to various types of complexes **IV**. The ^{1}H-NMR spectrum of the related dimethyl zirconocene system (Cp-*n*-Bu)$_2ZrMe_2$/MAO ([(Cp-*n*-Bu)$_2ZrMe_2$] = 0.01 M, Al/Zr = 60) exhibits two sharp pseudotriplets originating from **III** ($\delta = 5.66$, t and 5.68, t, $J_{HH} = 2.5$ Hz) and several broad signals originating from complexes $\mathbf{IV}_1$, $\mathbf{IV}_2$ and $\mathbf{IV}_3$ at 6.05, 5.93 and 5.85 ppm, respectively. The ^{13}C-NMR spectrum of the sample in Fig. 1a exhibits sharp peaks at 116.47 and 115.87 ppm from complex **III** and several broad peaks from complexes $\mathbf{IV}_1$, $\mathbf{IV}_2$ and $\mathbf{IV}_3$ in the range 112–114 ppm. Since the same signals have been observed also in the ^{13}C-NMR spectrum of the system (Cp-*n*-Bu)$_2ZrMe_2$/MAO at [(Cp-*n*-Bu)$_2ZrMe_2$] = 0.01 M, Al/Zr = 60, similar complexes **III** and **IV** are likely to be present in the systems (Cp-*n*-Bu)$_2ZrMe_2$/MAO and (Cp-*n*-Bu)$_2ZrCl_2$/MAO. For complex **II** observed for the (Cp-*n*-Bu)$_2ZrMe_2$/MAO system at Al/Zr = 10, sharp peaks of Cp carbons at 112.8 and 112.7 ppm were detected.

In contrast to the (Cp-*n*-Bu)$_2ZrCl_2$/MAO system, only one broad resonance has been detected for the Cp rings of **IV** in the ^{1}H- and ^{13}C-NMR spectra of the Cp_2ZrCl_2/MAO system [7]. Thus, substitution of the Cp ligands allows the resonances of complexes **IV** with differing counteranions of the type $[Me\text{-}MAO]^-$ to be observed separately. Recently, experimental evidences in favor of formation of $[Me\text{-}MAO]^-$ anions with different Lewis basicities in Cp_2ZrMe_2/MAO system were presented [17].

The sample with the same Al/Zr ratio as in Fig. 1a but with lower concentration of zirconocene ([(Cp-*n*-Bu)$_2ZrCl_2$] = 0.001 M) displays broad, poorly defined signals (Fig. 1b). In the sample of Fig. 1b, the peak of complex **III** is relatively small. This demonstrates that dilution of such a reaction system may disfavor formation of **III** due to a decrease in the concentration of Al_2Me_6. The intense broad peak at 5.76 ppm (Fig. 2b) was tentatively assigned to Cp hydrogen atoms of the monomethylated complex (Cp-*n*-Bu)$_2ZrMeCl$ (see Table 1).

The observed picture is simplified when the Al/Zr ratio is increased. Complex **III** becomes the predomi-

Table 3
Ethylene polymerization over (Cp-R)$_2ZrCl_2$/MAO catalysts (R = H, Me, *n*-Bu, *t*-Bu)

R	$Al_{(MAO)}/Zr$	C_2H_4 pressure (atm)	Polyethylene (PE) yield [a]		Initial activity [b] (kg of PE per mol Zr min atm C_2H_4)
			g	kg of PE per mol of Zr	
H	200	2	7.7	3850	255
Me	200	5	5.2	2600	60
n-Bu	200	2	0.7	350	35
t-Bu	200	5	0.1	50	–
H	1000	2	17.1	8550	610
Me	1000	2	14.3	7150	320
n-Bu	1000	2	23.4	11700	460
t-Bu	1000	5	7.5	3750	92

[a] PE yield per 15 min.
[b] Initial activity calculated from the PE yield per 5 min.

Table 4
^{1}H-NMR signals of $[(Cp\text{-}R)_2Zr(\mu\text{-}Me)_2AlMe_2]^+[Me\text{-}MAO]^-$ (**III**) and $[(Cp\text{-}R)_2Zr(\mu\text{-}Me)_2AlMe_2]^+[B(C_6F_5)_4]^-$ complexes (R = 1,2-Me_2, 1,2,3-Me_3, 1,2,4-Me_3, Me_4)

Species	Cp	Cp-Me	μ-Me	Al-Me
$[(Cp\text{-}1,2\text{-}Me_2)_2Zr(\mu\text{-}Me)_2AlMe_2]^+[Me\text{-}MAO]^-$	5.57 (d, 4), 5.45 (t, 2), J_{HH} = 2.9 Hz	1.49 (s, 12)	NF	−0.64 (s, 6)
$[(Cp\text{-}1,2,3\text{-}Me_3)_2Zr(\mu\text{-}Me)_2AlMe_2]^+[Me\text{-}MAO]^-$	5.36 (s, 4)	1.40 (s, 12), 1.53 (s, 6)	−0.51 (s, 6)	−0.62 (s, 6)
$[(Cp\text{-}1,2,4\text{-}Me_3)_2Zr(\mu\text{-}Me)_2AlMe_2]^+[Me\text{-}MAO]^-$	5.42 (s, 4)	1.42 (s, 12), 1.46 (s, 6)	−0.50 (s, 6)	−0.61 (s, 6)
$[(Cp\text{-}Me_4)_2Zr(\mu\text{-}Me)_2AlMe_2]^+[Me\text{-}MAO]^-$	5.54 (s, 2)	1.38 (s, 12), 1.49 (s, 12)	−0.59 (s, 6)	−0.62 (s, 6)
$[(Cp\text{-}1,2\text{-}Me_2)_2Zr(\mu\text{-}Me)_2AlMe_2]^+[B(C_6F_5)_4]^-$	5.40 (d, 4), 5.29 (t, 2), J_{HH} = 2.9 Hz		−0.48 (s, 6)	−0.70 (s, 6)
$[(Cp\text{-}1,2,3\text{-}Me_3)_2Zr(\mu\text{-}Me)_2AlMe_2]^+[B(C_6F_5)_4]^-$	5.26 (s, 4)	1.48 (s, 12), 1.53 (s, 6)	NF	−0.70 (s, 6)
$[(Cp\text{-}1,2,4\text{-}Me_3)_2Zr(\mu\text{-}Me)_2AlMe_2]^+[B(C_6F_5)_4]^-$	5.37 (s, 4)	1.38 (s, 12), 1.53 (s, 6)	NF	−0.66 (s, 6)
$[(Cp\text{-}Me_4)_2Zr(\mu\text{-}Me)_2AlMe_2]^+[B(C_6F_5)_4]^-$	5.37 (s, 2)	1.39 (s, 12), 1.49 (s, 12)	NF	−0.44 (s, 6)

NF, not found.

nant species at the higher Al/Zr ratios (Figs. 1d and e). Two pseudotriplets are characteristics of the Cp hydrogen atoms of **III** (Fig. 1a). The distance between these pseudotriplets decreases with diminishing zirconocene concentration. No significant difference assignable to the presence of different $[Me\text{-}MAO]^-$ anions at different Al/Zr ratios could be detected in the ^{1}H-NMR spectra of the outer-sphere ion pair **III**.

The Al/Zr ratios in samples of Figs. 1b–e were changed by the decrease in the amount of (Cp-*n*-$Bu)_2ZrCl_2$ at constant concentration of MAO. We have also made experiments at constant concentration of (Cp-*n*-$Bu)_2ZrCl_2$, while Al/Zr ratio was changed by varying the amount of MAO. In this case, complex **III** also dominated at high Al/Zr ratios. However, in contrast to the samples in Figs. 1b–e, pseudotriplets corresponding to **III** resolved nicely (Fig. 2). In the first case (Fig. 1), toluene-d_8 solution of solid MAO was stored several days at room temperature before preparation of samples; in the second case (Fig. 2), appropriate amount of solid MAO was added into the solution of (Cp-*n*-$Bu)_2ZrCl_2$ in d_8-toluene just before recording the NMR spectra. Thus, in order to obtain well-resolved NMR spectra of **III**, prolonged storing of toluene solutions of solid MAO should be avoided.

The polymerization data show that the catalytic system (Cp-*n*-$Bu)_2ZrCl_2$/MAO is virtually inactive at Al/Zr ratios lower than 200. Polymerization activity at an Al/Zr ratio of 1000 is higher by a factor of 13 than that at Al/Zr = 200 (Table 3). According to the NMR experiments, the concentration of species **III** increases at the expense of species **IV** with the increase of Al/Zr ratio. Despite the concentration of zirconocene under conditions of polymerization experiment is by 1–2 order of magnitude lower, it is natural to expect that the portion of **III** in polymerization experiment will also

Table 5
Ethylene polymerization over $(Cp\text{-}R)_2ZrCl_2$/MAO catalysts

R	$Al_{(MAO)}$/Zr	C_2H_4 pressure (atm)	PE yield [a]		Initial activity [b] (kg of PE per mol Zr min atm C_2H_4)
			g	kg of PE per mol of Zr	
H	200	2	7.7	3850	255
Me	200	5	5.2	2600	60
1,2-Me_2	200	2	13.0	6500	470
1,2,3-Me_3	200	5	10.0	5000	102
1,2,4-Me_3	200	5	13.9	6950	134
Me_4	200	5	17.1	8550	190
Me_5	200	5	11.5	5750	145
$Me_2Si(Ind)_2$	200	2	15.6	7800	420
H	1000	2	17.1	8550	610
Me	1000	2	14.3	7150	320
1,2-Me_2	1000	2	19.0	9500	520
1,2,3-Me_3	1000	5	8.6	4300	115
1,2,4-Me_3	1000	2	8.7	4350	232
Me_4	1000	2	11.6	5800	300
Me_5	1000	2	14.1	7050	445
$Me_2Si(Ind)_2$	1000	2	16.0	8000	450

[a] PE yield per 15 min.
[b] Initial activity calculated from the PE yield per 5 min.

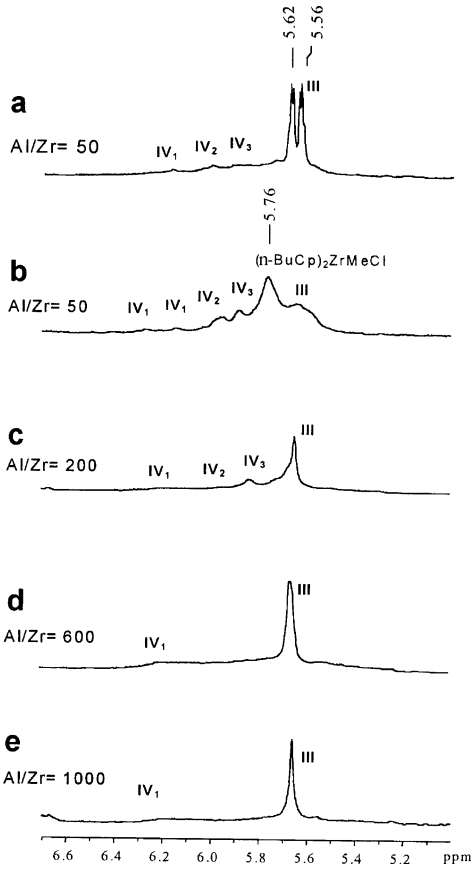

Fig. 1. ^{1}H-NMR spectra (in the range of Cp hydrogen atoms, at 20 °C) of the system (Cp-*n*-Bu)$_2$ZrCl$_2$/MAO at Al/Zr ratios of 50 (a), 50 (b), 200 (c), 600 (d) and 1000 (e). Sample (a): [MAO] = 1.5 M, [(Cp-*n*-Bu)$_2$ZrCl$_2$] = 3×10^{-2} M; samples (b)–(e): [MAO] = 0.5 M; [(Cp-*n*-Bu)$_2$ZrCl$_2$] = 10^{-2} M (b), 2.5×10^{-3} M (c), 8×10^{-4} M (d) and 5×10^{-4} M (e).

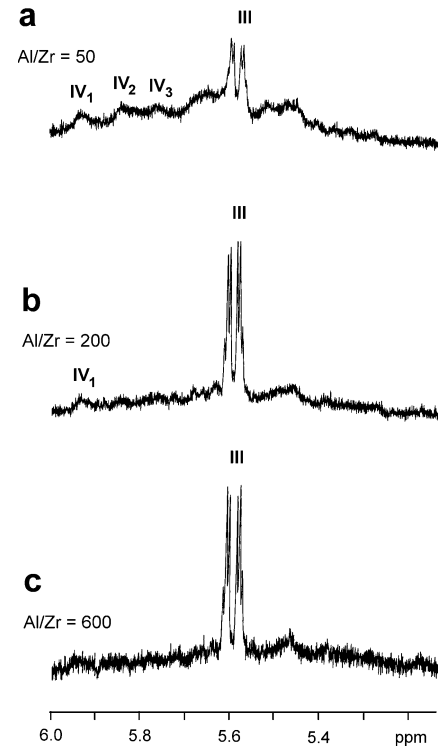

Fig. 2. ^{1}H-NMR spectra (in the range of Cp hydrogen atoms) of the system (Cp-*n*-Bu)$_2$ZrCl$_2$/MAO at Al/Zr ratios of 50 (a), 200 (b) and 600 (c). [(Cp-*n*-Bu)$_2$ZrCl$_2$] = 10^{-3} M (b); [MAO] = 0.05 M (a), 0.2 M (b) and 0.6 M (c).

increase with the growth of Al/Zr ratio. Thus, we assign the increase in catalytic activity of (Cp-*n*-Bu)$_2$ZrCl$_2$/MAO system with the increment of Al/Zr ratio mainly to the increase of concentrations of species of type **III**.

3.1.2. (Cp-t-Bu)$_2$ZrCl$_2$/MAO

Like for the case of R = *n*-Bu, the zirconocene species present in these reaction systems at various Al/Zr ratios were monitored mainly by ^{1}H-NMR spectroscopy (Fig. 3, Table 2). At Al/Zr = 50, the initial complex (Cp-*t*-Bu)$_2$ZrCl$_2$ and the monomethylated complex (Cp-*t*-Bu)$_2$ZrClMe are the major species, while the concentrations of complexes **III** and **IV** are low (Fig. 3a). The ratio of the zirconium complexes of the sample in Fig. 3a did not vary substantially within a day at room temperature.

At Al/Zr = 200, the ^{1}H-NMR spectrum of the system (Cp-*t*-Bu)$_2$ZrCl$_2$/MAO displays the intense peaks of complex **III** (R = *t*-Bu) with partially resolved spin–spin splitting $J_{HH} = 2.6$ Hz. The remaining signals marked as **IV**$_1$, **IV**$_2$ and **IV**$_3$ were assigned to complexes of type **IV**. The H,H-COSY spectra displayed no

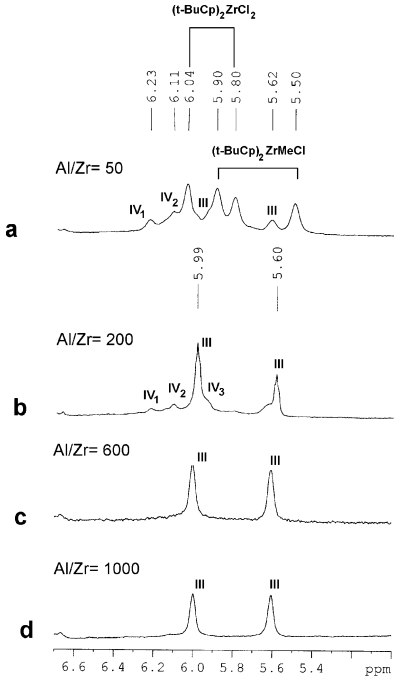

Fig. 3. ^{1}H-NMR spectra (in the range of Cp hydrogen atoms, at 20 °C) of the system (Cp-*t*-Bu)$_2$ZrCl$_2$/MAO at Al/Zr ratios of 50 (a), 200 (b), 600 (c) and 1000 (d). [MAO] = 0.5 M; [(Cp-*t*-Bu)$_2$ZrCl$_2$] = 10^{-2} M (a), 2.5×10^{-3} M (b), 8×10^{-4} M (c) and 5×10^{-4} M (d).

correlation between the signals of $\mathbf{IV}_1$ and $\mathbf{IV}_2$. These signals are thus likely to originate from distinct complexes.

Further increase of the Al/Zr ratio up to 600–1000 causes a drop in concentrations of complexes **IV** such that complex **III** is now predominantly present (Figs. 3c and d). This result differs from that for Cp_2ZrMe_2/MAO system where complexes **III** and **IV** were present in comparable concentrations even at Al/Zr ratio of 1000 [7]. Probably, the bulky *t*-Bu substituents disfavor the anion–cation contacts in complex **IV**, and thus formation of species **III** with outer-sphere counterion becomes preferable. Practically, all starting complex (Cp-*t*-Bu)$_2$ZrCl$_2$ converts into species **III** upon interaction with MAO at Al/Zr ratio higher than 500.

As for R = *n*-Bu, the presence of different counteranions in **III** (R = *t*-Bu) does not give rise to any significant differences in the ^{1}H-NMR spectra of **III** (Figs. 3b–d). Apparently, ^{1}H-NMR spectra of **III** are not as sensitive to variations in the nature of their [Me-MAO]$^-$ counteranions as the ^{1}H-NMR spectra of the ion pair **IV**, since in **III** the perturbing [Me-MAO]$^-$ anion is only in outer-sphere contact to the coordinatively saturated zirconocene cation. Besides, [Me-MAO]$^-$ anions can rapidly exchange between various species **III**, and thus the cationic part of **III** displays one sharp NMR pattern.

As for R = *n*-Bu, the polymerization activity of the (Cp-*t*-Bu)$_2$ZrCl$_2$/MAO system at Al/Zr ratio of 1000 is much higher than that at Al/Zr = 200 (Table 3). The data in Table 3 would thus indicate that outer-sphere ion pairs of the type **III** (or their polymeryl homologs) are the immediate precursors for the crucial alkyl zirconocene olefin cations required for polymer growth.

3.1.3. *(Cp-Me)$_2$ZrCl$_2$/MAO*

Fig. 4 shows ^{1}H-NMR spectra (range of Cp hydrogen atoms) of the catalytic system (Cp-Me)$_2$ZrCl$_2$/MAO. It is seen that at Al/Zr = 50 only very broad peaks are observed. None of them can be attributed to complex **III** (Fig. 4b). With the increase of Al/Zr ratio, the relative intensity of the resonance of complex **III** grows (Fig. 4c). Two pseudotriplets, which can be expected for Cp protons of complex **III**, are not resolved and only one broadened peak is observed, whereas the related ion pair $[(\text{Cp-Me})_2\text{Zr}(\mu\text{-Me})_2\text{AlMe}_2]^+[\text{B}(\text{C}_6\text{F}_5)_4]^-$ displays two pseudotriplets (Table 2). The origin of the exchange process leading to this effect is still unclear. For all other zirconocenes studied in this work, well-resolved ^{1}H-NMR spectra of **III** could be obtained.

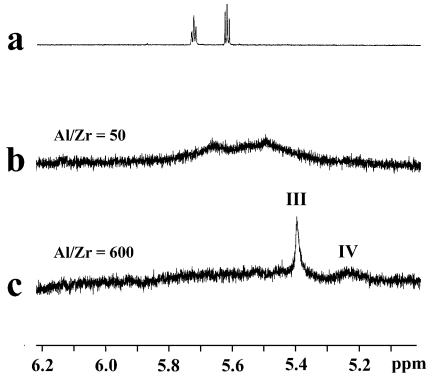

Fig. 4. ^{1}H-NMR spectra (in the range of Cp hydrogen atoms, at 20 °C) of the system (Cp-Me)$_2$ZrCl$_2$/MAO: before addition of MAO (a); at Al/Zr ratios of 50 (b) and 600 (c). [(Cp-*t*-Bu)$_2$ZrCl$_2$] = 10^{-3} M; [MAO] = 5×10^{-2} M (b) and 0.6 M (c).

The polymerization activity of the (Cp-Me)$_2$ZrCl$_2$/MAO system at an Al/Zr ratio of 1000 is higher by a factor of 5 than that at an Al/Zr ratio of 200. This increase of activity is noticeably lower than that for R = *n*-Bu and *t*-Bu but is rather close to the corresponding increase for R = H (Table 3).

To summarize the results of this chapter, one can conclude that, for (Cp-R)$_2$ZrCl$_2$/MAO systems (R = Me, *n*-Bu, *t*-Bu), the relative concentration of **III** grows with increasing Al/Zr ratios. In the case of R = *t*-Bu, only complex **III** is observed in the reaction solution at an Al/Zr ratio of more than 500. Probably, the bulky *t*-Bu substituents disfavor the anion–cation contacts in complex **IV** and thus formation of species **III** with outer-sphere counterion becomes preferable. Complexes **IV** (R = Me, *n*-Bu, *t*-Bu) with different [Me-MAO]$^-$ counteranions can display distinct ^{1}H- and ^{13}C-NMR peaks, whereas NMR spectra of **III** are not as sensitive to variations in the nature of their [Me-MAO]$^-$ counteranions. Polymerization activity for R = *t*-Bu is noticeably lower than for R = *n*-Bu and Me, probably due to a negative effect of the bulkiness of R.

3.2. *Spectroscopic and polymerization study of the catalytic systems (Cp-R)$_2$ZrCl$_2$/MAO (R = Me, 1,2-Me$_2$, 1,2,3-Me$_3$, 1,2,4-Me$_3$, Me$_4$)*

In order to elucidate the effect of the number of methyl substituents on the relative concentration of species **III** and **IV**, and on the polymerization activity, spectroscopic and polymerization data for catalytic systems (Cp-R)$_2$ZrCl$_2$/MAO (R = Me, 1,2-Me$_2$, 1,2,3-Me$_3$, 1,2,4-Me$_3$, Me$_4$) were compared at various Al/Zr ratios. More detailed experimental data were obtained for the (Cp-1,2,3-Me$_3$)$_2$ZrCl$_2$/MAO system.

The ^{1}H-NMR spectrum of the system (Cp-1,2,3-Me$_3$)$_2$ZrCl$_2$/MAO at Al/Zr = 50 (in the range of Cp hydrogen atoms) exhibits the signal of complex **III** (R = 1,2,3-Me$_3$) and several weaker signals (Fig. 5a, Table 4). None of these can be assigned to the monomethylated complex (Cp-1,2,3-Me$_3$)$_2$ZrClMe (Table 1). A H,H-COSY spectrum shows that the two sharp doublets at 5.60 and 5.01 ppm in Fig. 3a belong to one and the same still unidentified complex. The remaining broad signals can be assigned to complexes **IV** (R = 1,2,3-Me$_3$).

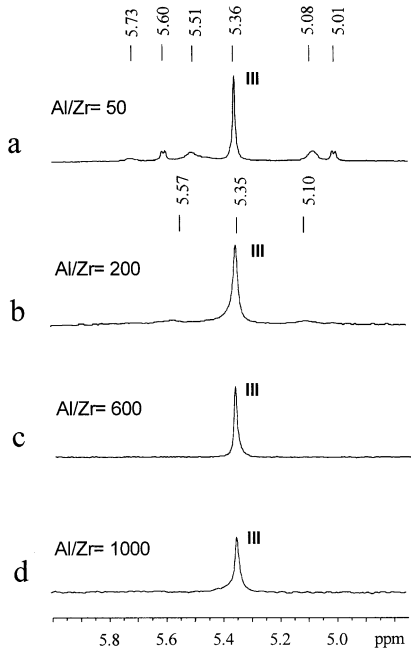

Fig. 5. ^{1}H-NMR spectra (in the range of Cp hydrogen atoms, at 20 °C) of the system (Cp-1,2,3-Me_3)$_2$$ZrCl_2$/MAO in toluene-$d_8$ at various Al/Zr ratios: 50 (a), 200 (b), 600 (c) and 1000 (d). [MAO] = 0.5 M; [(Cp-1,2,3-Me_3)$_2$$ZrCl_2$] = 10^{-2} M (a), 2.5×10^{-3} M (b), 8×10^{-4} M (c) and 5×10^{-4} M (d).

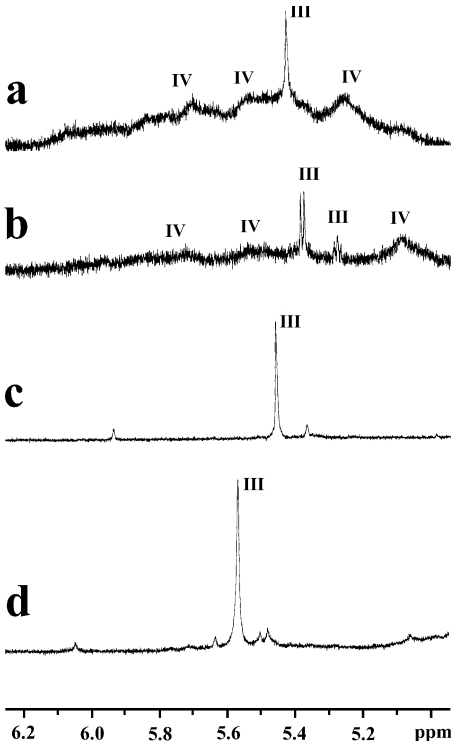

Fig. 6. ^{1}H-NMR spectra of (Cp-R)$_2$$ZrCl_2$/MAO systems in toluene (at 20 °C, Al/Zr = 200, [(Cp-R)$_2$$ZrCl_2$] = 10^{-3} M): R = Me (a), R = 1,2-Me_2 (b), R = 1,2,4-Me_3 (c) and R = Me_4 (d).

In contrast to the systems (Cp-R)$_2$$ZrCl_2$/MAO (R = Me, *n*-Bu, *t*-Bu), complex **III** dominates in the system (Cp-1,2,3-Me_3)$_2$$ZrCl_2$/MAO even at an Al/Zr ratio of 50. At higher Al/Zr ratios (Figs. 5c and d), complex **III** is the only one observable in the reaction solution, as was the case also for R = *t*-Bu. Again in distinction to the systems (Cp-R)$_2$$ZrCl_2$/MAO (R = Me, *n*-Bu, *t*-Bu), the polymerization activity of the system (Cp-1,2,3-Me_3)$_2$$ZrCl_2$/MAO was constant in the range of Al/Zr ratios 200–1000 (Table 5).

Complex **III** (R = 1,2,3-Me_3) appears to be stabilized relative to the contact ion pair **IV** by the more highly substituted Cp ligands. To elucidate the effect of Me substituents on the relative concentrations of complexes **III** and **IV**, ^{1}H-NMR spectra of the catalytic systems (Cp-R)$_2$$ZrCl_2$/MAO (R = Me, 1,2-$Me_2$, 1,2,3-$Me_3$, 1,2,4-$Me_3$, Me_4) were compared at the same zirconocene concentrations and Al/Zr ratios. As an example, Fig. 6 shows ^{1}H-NMR spectra (the range of Cp hydrogen atoms) of (Cp-R)$_2$$ZrCl_2$/MAO systems (R = Me, 1,2-Me_2, 1,2,4-Me_3, Me_4; [(Cp-R)$_2$$ZrCl_2$] = 0.001 M; Al/Zr = 200). It is seen that in the case of R = Me and 1,2-Me_2, broad signals of complexes **IV** are present in the reaction solution at Al/Zr of 200, whereas in the case of R = 1,2,4-Me_3 and Me_4, only the sharp peaks of complexes **III** are observed. Thus, three or four Me substituents in a Cp ring stabilize **III** relative to **IV** in (Cp-R)$_2$$ZrCl_2$/MAO systems.

According to ^{1}H-NMR spectroscopic data, only complex **III** is present in the catalytic systems (Cp-R)$_2$$ZrCl_2$/MAO (R = 1,2,3-$Me_3$, 1,2,4-$Me_3$, Me_4) at Al/Zr = 200. Thus, one should expect that their catalytic activity should be close at Al/Zr of 200 and 1000, since the starting complex entirely converts into active species **III** even at Al/Zr of 200. Indeed, the polymerization data for (Cp-R_n)$_2$$ZrCl_2$/MAO (R = 1,2,3-$Me_3$, 1,2,4-$Me_3$, Me_4) systems at Al/Zr = 200 and 1000 (Table 5) show that with the growth of Al/Zr ratios from 200 to 1000 the activities of these systems are almost constant.

For the catalytic systems (Cp-R)$_2$$ZrCl_2$/MAO (R = H, Me, 1,2-$Me_2$, *n*-Bu, *t*-Bu), besides the sharp peaks of **III**, broad signals of complexes **IV** are observed in the ^{1}H-NMR spectra of the reaction solutions at Al/Zr of 200. Thus, one can expect that the activity of these systems would go up with the increase of Al/Zr ratio due to a decrease of the concentration of complexes **IV** and a corresponding increase of that of the more active complex **III**. This prediction is valid for R = H, Me, *n*-Bu, *t*-Bu (Table 3). However, the activity of the (Cp-1,2-Me_2)$_2$$ZrCl_2$/MAO system is almost the same at Al/Zr of 200 and 1000 (Table 5). Probably, in this particular case the activities of species **III** and **IV** are comparable. Further studies are needed to verify this assumption. Despite this exception, complex **III** seems to be the main precursor of the active centers of polymerization for the catalytic systems studied. The data obtained for the

Table 6
Ethylene polymerization over (Cp-R)$_2$ZrCl$_2$/AlMe$_3$/[Ph$_3$C][B(C$_6$F$_5$)$_3$] catalysts (Zr:Al:B = 1:100:1)

Zirconocene	PE yield		Initial activity (kg PE per mol Zr min atm)
	g	kg PE per mol Zr	
Cp$_2$ZrCl$_2$	0.70	700	28.0
(Cp-Me)$_2$ZrCl$_2$	0.61	610	30.7
(Cp-1,2-Me$_2$)$_2$ZrCl$_2$	0.60	600	30.0
(Cp-1,2,3-Me$_3$)$_2$ZrCl$_2$	0.75	750	30.0
(Cp-1,2,4-Me$_3$)$_2$ZrCl$_2$	0.93	930	42.0
(Cp-Me$_4$)$_2$ZrCl$_2$	0.84	840	37.3
(Cp-Me$_5$)$_2$ZrCl$_2$	1.95	1950	100.0
(Cp-*t*-Bu)$_2$ZrCl$_2$	0.93	930	42.0
(Cp-*n*-Bu)$_2$ZrCl$_2$	1.65	1650	70.0
Me$_2$Si(Ind)$_2$ZrCl$_2$	3.72	3720	200.7

Polymerization conditions: $T = 50$ °C, C_2H_4 pressure = 3 atm, in toluene for 15 min, [Zr] = 1.4×10^{-5} M.

systems (Cp-R)$_2$ZrCl$_2$/MAO correlate with those for the highly active catalytic systems (Cp-R)$_2$ZrCl$_2$/AlMe$_3$/CPh$_3^+$B(C$_6$F$_5$)$_4^-$ (Table 6). In the latter, ^{1}H-NMR spectroscopy indicates the presence of only the intermediates [(Cp-R)$_2$ZrMe(μ-Me)$_2$AlMe$_2$]$^+$[B(C$_6$F$_5$)$_4$]$^-$ containing the same cations as those in the intermediates **III** in the MAO-based systems, thus confirming the role of complex **III** as the precursor of the crucial catalyst species.

In conclusion, three or four Me substituents in a Cp ring stabilize **III** relative to **IV** in (Cp-R)$_2$ZrCl$_2$/MAO systems (**III** dominates in reaction solution even at Al/Zr of 50–100). As a result, the polymerization activity of (Cp-R$_n$)$_2$ZrCl$_2$/MAO systems (R = 1,2,3-Me$_3$, 1,2,4-Me$_3$, Me$_4$) is virtually constant in the range of Al/Zr ratios 200–1000.

3.3. Spectroscopic study of L_2ZrCl_2/MAO systems (L_2 are various indenyl and fluorenyl ligands)

In order to exceed spectroscopic monitoring of active species of polymerization to more complex and practically attractive zirconocene catalysts, catalytic systems L$_2$ZrCl$_2$/MAO (L$_2$ are various indenyl and fluorenyl ligands) were studied.

The analysis of ^{1}H-NMR spectra of the L$_2$ZrCl$_2$/MAO systems shows that for all catalysts studied (L$_2$ZrCl$_2$ = rac-ethanediyl(Ind)$_2$ZrCl$_2$, rac-Me$_2$Si(Ind)$_2$ZrCl$_2$, rac-Me$_2$Si(1-Ind-2-Me)$_2$ZrCl$_2$, rac-ethanediyl(1-Ind-4,5,6,7-H$_4$)$_2$ZrCl$_2$, (Ind-2-Me)$_2$ZrCl$_2$, Me$_2$C(Cp)(Flu)ZrCl$_2$, Me$_2$C(Cp-3-Me)(Flu)ZrCl$_2$, Me$_2$Si(Flu)$_2$ZrCl$_2$), broad resonances of **IV** were not detected at all or were observed only at low Al/Zr ratios (50–100), whereas only the 'cation-like' complex [L$_2$Zr(μ-Me)$_2$AlMe$_2$]$^+$[Me-MAO]$^-$ (**III**) was observed in the reaction solution at Al/Zr ratios of 200–500. Probably, the substituents and bulkiness of the ligands disfavor the anion–cation contacts in complex **IV** due to steric or electronic effects. Complexes **III** exhibit sharp ^{1}H-NMR resonances ($\Delta\vartheta_{1/2} = 0.5$ Hz) that simplify their detection even in the presence of large excess of MAO. As an example, the ^{1}H-NMR spectrum of complex **III** observed in the system rac-ethanediyl(Ind)$_2$ZrCl$_2$/MAO at an Al/Zr ratio of 300 is presented in Fig. 7. A spin–spin coupling constant of 0.7 Hz is resolved for one of the Ind-C$_5$ protons of **III**. Complexes **III** are stable for weeks at 20 °C in the samples studied. The ^{1}H-NMR parameters of 'cation-like' species **III** for the systems investigated are collected in Tables 7 and 8 in comparison with the data available for the corresponding complexes [L$_2$Zr(μ-Me)$_2$AlMe$_2$]$^+$[B(C$_6$F$_5$)$_4$]$^-$ and [L$_2$Hf(μ-Me)$_2$AlMe$_2$]$^+$[B(C$_6$F$_5$)$_4$]$^-$, detected in CPh$_3^+$B(C$_6$F$_5$)$_4^-$-based systems [15]. It is seen that, despite the nonuniformity of their [Me-MAO]$^-$ counterions, the cationic parts of complexes **III** can be characterized by ^{1}H-NMR spectroscopy equally well as for related complexes in reaction systems based on CPh$_3^+$B(C$_6$F$_5$)$_4^-$.

Ethylene polymerization data were obtained only for the system rac-Me$_2$Si(Ind)$_2$ZrCl$_2$/MAO (Table 5). As can be expected, the polymerization activity of this system was constant at Al/Zr ratios of 200–1000, since

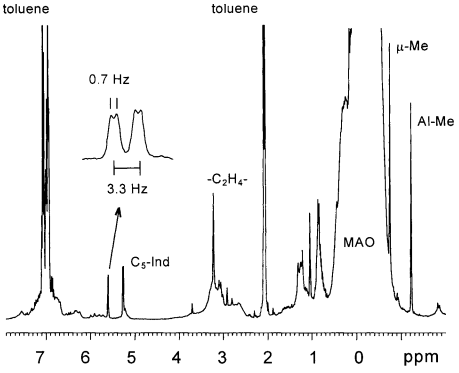

Fig. 7. ^{1}H-NMR spectrum of [ethanediyl(Ind)$_2$Zr(μ-Me)$_2$Al-Me$_2$]$^+$[Me-MAO]$^-$ in toluene at 20 °C ([Zr] = 3×10^{-3} M, Al/Zr = 300).

Table 7
^{1}H-NMR signals of complexes [rac-R_1(Ind-R)$_2$Zr(μ-Me)$_2$AlMe$_2$]$^+$[Me-MAO]$^-$ and [rac-R_1(Ind)$_2$Zr(μ-Me)$_2$AlMe$_2$]$^+$[B(C_6F_5)$_4$]$^-$ (R = H, 2-Me; R_1 = none, $-C_2H_4-$, $-SiMe_2-$)

Species	Ind-C_5	$-C_2H_4-$	$-SiMe_2-$	μ-Me	Al-Me
[rac-ethanediyl(Ind)$_2$Zr(μ-Me)$_2$AlMe$_2$]$^+$[B(C_6F_5)$_4$]$^-$ [a]	6.44 (dd, 2), J = 3.3 and 0.7 Hz; 6.20 (d, 2), J = 3.3 Hz	4.04 (s, 4)		−0.58 (s, 6)	−0.63 (s, 6)
[rac-Me$_2$Si(Ind)$_2$Zr(μ-Me)$_2$AlMe$_2$]$^+$[B(C_6F_5)$_4$]$^-$ [a]	6.92 (d, 2), J = 3.3 Hz; 5.91 (d, 2), J = 3.3 Hz		1.29 (s, 6)	−0.61 (s, 6)	−0.81 (s, 6)
[rac-ethanediyl(Ind)$_2$Zr(μ-Me)$_2$AlMe$_2$]$^+$[Me-MAO]$^-$ [b]	5.61 (dd, 2), J = 3.3 and 0.7 Hz; 5.26 (d, 2), J = 3.3 Hz	3.22 (s, 4)		−0.75 (s, 6)	−1.22 (s, 6)
[rac-Me$_2$Si(Ind)$_2$Zr(μ-Me)$_2$AlMe$_2$]$^+$[Me-MAO]$^-$ [b]	6.16 (d, 2), J = 3.3 Hz; 5.03 (d, 2), J = 3.3 Hz		0.85 (s, 6)	−0.65 (s, 6)	−1.35 (s, 6)
[rac-Me$_2$Si(1-Ind-2-Me)$_2$Zr(μ-Me)$_2$AlMe$_2$]$^+$[Me-MAO]$^-$ [b,c]	5.86 (s, 2)		0.9 (s, 6)	−0.65 (s, 6)	−1.39 (s, 6)
[(2-Me-Ind)$_2$Zr(μ-Me)$_2$AlMe$_2$]$^+$[Me-MAO]$^-$ [b,d]	5.80 (s, 4)			−0.53 (s, 6)	−1.1 (s, 6)
[rac-ethanediyl(1-Ind-4,5,6,7-H_4)$_2$Zr(μ-Me)$_2$AlMe$_2$]$^+$[Me-MAO]$^-$	5.48 (d, 2), J = 2.9 Hz; 4.76 (d, 2), J = 2.9 Hz	2.84 (m, 2), 2.57 (m, 2)		−0.26 (s, 6)	−0.62 (s, 6)

[a] In CD_2Cl_2 at 20 °C [15].
[b] In toluene-d_8 at 20 °C.
[c] 2-Me peak at 1.53 (s, 6).
[d] 2-Me peak at 1.82 (s, 6).

the starting complex is entirely converted to the active species **III** even at an Al/Zr ratio of 100.

We also tried to monitor the concentration of **III** directly in the course of 1-hexene polymerization by rac-Me$_2$Si(Ind)$_2$ZrCl_2/MAO. In particular, 1-hexene was added at −25 °C to an NMR tube containing only species **III** as a catalyst ([rac-Me$_2$Si(Ind)$_2$ZrCl_2] = 0.001 M, Al/Zr = 100, [1-hexene] = 0.01 M). Upon warming the sample to 10 °C, ^{1}H-NMR spectra indicate that 1-hexene is converted to the corresponding polymer with a characteristic time of 5 min. However, the ^{1}H-NMR peaks of **III** remained unchanged. Thus, the conditions of this experiment are not suitable for detection of polymeryl homologs of **III**. Probably, $AlMe_3$ present in excess rapidly displaces polymeryl ligands to restore **III**. Nevertheless, this experiment shows that a catalytic system, which contains only species **III** as a catalyst, is able to polymerize 1-hexene.

In conclusion, the analysis of ^{1}H-NMR spectra of the L_2ZrCl_2/MAO systems, where L_2 are various indenyl and fluorenyl ligands, shows that for all catalysts studied, broad resonances of **IV** were not detected at all or were observed only at low Al/Zr ratios (50–100), whereas only the 'cation-like' complex [L_2Zr(μ-Me)$_2$AlMe$_2$]$^+$[Me-MAO]$^-$ (**III**) was observed in the reaction solution at Al/Zr ratios of 200–500. Despite the non-uniformity of their [Me-MAO]$^-$ counterions, the cationic parts of complexes **III** can be characterized by ^{1}H-NMR spectroscopy equally well as for related complexes in reaction systems based on $CPh_3^+B(C_6F_5)_4^-$.

Table 8
^{1}H-NMR signals of complexes [Me$_2$C(Cp)(Flu)Hf(μ-Me)$_2$AlMe$_2$]$^+$[B(C_6F_5)$_4$]$^-$, [Me$_2$C(Cp-R)(Flu)Zr(μ-Me)$_2$AlMe$_2$]$^+$[Me-MAO]$^-$ and [Me$_2$Si(Flu)$_2$Zr(μ-Me)$_2$AlMe$_2$]$^+$[Me-MAO]$^-$ (R = H, 3-Me)

Species	Flu	C_5	$-CMe_2-$	μ-Me	Al-Me
[Me$_2$C(Cp)(Flu)Hf(μ-Me)$_2$AlMe$_2$]$^+$[B(C_6F_5)$_4$]$^-$ [a]	8.22 (d, 2), J = 8.58 Hz; 7.96 (d, 2), J = 8.91 Hz; 7.75 (t, 2), J = 8.58 Hz; 7.34 (t, 2), J = 8.91 Hz	6.32 (t, 2), J = 2.6 Hz; 5.58 (t, 2), J = 2.6 Hz	2.49 (s, 6)	−0.57 (s, 6)	−0.72 (s, 3), −0.63 (s, 3)
[Me$_2$C(Cp)(Flu)Zr(μ-Me)$_2$AlMe$_2$]$^+$[Me-MAO]$^-$	7.52 (d, 2), J = 8.5 Hz; 7.28 (t, 2), J = 8.5 Hz; 7.01 (t, 2), J = 8.5 Hz [b]	5.60 (t, 2), J = 2.6 Hz; 4.68 (t, 2), J = 2.6 Hz	1.89 (s, 6)	−0.76 (s, 6)	−1.51 (s, 6)
[Me$_2$C(3-Me-Cp)(Flu)Zr(μ-Me)$_2$AlMe$_2$]$^+$[Me-MAO]$^-$ [c]	7.57 (t, 2), J = 8.5 Hz [b]	5.55 (t, 2), J = 2.6 Hz; 5.31 (t, 1), J = 2.6 Hz	1.86 (s, 6)	−0.71 (s, 6)	−1.73 (s, 3), −1.57 (s, 3)
[Me$_2$Si(Flu)$_2$Zr(μ-Me)$_2$AlMe$_2$]$^+$[Me-MAO]$^-$ [d]	6.65 (t, 4), J = 8 Hz [b]			−0.72 (s, 6)	−2.46 (s, 6)

[a] [15].
[b] Masked by the signal of toluene.
[c] Peak of 3-Me at 1.92 (s, 6).
[d] Peak of Me_2Si at 1.37 (s, 6).

Acknowledgements

This work was supported by INTAS grant 00-0841. Funding from NTNU, under the Strategic Area: Materials Program, is acknowledged. The authors thank Dr. D.E. Babushkin for valuable discussions.

References

[1] E. Chen, T.J. Marks, Chem. Rev. 100 (2000) 1391.
[2] W. Kaminsky (Ed.), Metalorganic Catalysts for Synthesis and Polymerization: Recent Results by Ziegler-Natta and Metallocene Investigations, Springer-Verlag, Berlin, 1999.
[3] R.F. Jordan (Ed.), J. Mol. Catal. A: Chem. 128 (1998) N1–3 (special issue on metallocene and single site olefin catalysts).
[4] M. Bochmann, J. Chem. Soc. Dalton Trans. (1996) 255.
[5] H.-H. Brintzinger, D. Fischer, R. Mülhaupt, B. Rieger, R.M. Waymouth, Angew. Chem. Int. Ed. Engl. 34 (1995) 1143.
[6] I. Tritto, R. Donetti, C. Sacchi, P. Locatelli, G. Zannoni, Macromolecules 30 (1997) 1247.
[7] D.E. Babushkin, N.V. Semikolenova, V.A. Zakharov, E.P. Talsi, Macromol. Chem. Phys. 201 (2000) 558.
[8] V.A. Zakharov, I.I. Zakharov, Macromol. Theory Simul. 11 (2002) 352.
[9] J.C.W. Chien, A. Razavi, J. Polym. Sci. A 26 (1998) 2369.
[10] L.A. Nekhaeva, G.N. Bondarenko, S.V. Rykov, A.I. Nekhaev, B.A. Krentsel, V.P. Mar'in, L.I. Vyshinskaya, L.M. Khrapova, A.V. Polonskii, N.N. Korneev, J. Organomet. Chem. 406 (1991) 139.
[11] C. Janiak, K.C.H. Lange, U. Versteeg, D. Lentz, P.H.M. Budzelaar, Chem. Ber. 129 (1996) 1517.
[12] R. Kleinschmidt, Y. van der Leek, M. Reffke, G. Fink, J. Mol. Catal. A: Chem. 148 (1999) 29.
[13] I. Tritto, D. Zucchi, M. Destro, M.C. Sacchi, T. Dall'Occo, M. Galimberti, J. Mol. Catal. A: Chem. 160 (2000) 107.
[14] N.E. Grimmer, N.J. Coville, C.B. de Koning, J. Mol. Catal. A: Chem. 188 (2002) 105.
[15] M. Bochmann, S.J. Lancaster, Angew. Chem. Int. Ed. Engl. 33 (1994) 1634.
[16] J. Zhou, S.L. Lancaster, D.A. Walker, S. Beck, M. Thornton-Pett, M. Bochmann, J. Am. Chem. Soc. 123 (2001) 223.
[17] D.E. Babushkin, H.H. Brintzinger, J. Am. Chem. Soc. 124 (2002) 12869.